Voltage Fluctuations in ac Biased Superconducting Transition-Edge Sensors

L. Gottardi,* M. de Wit, E. Taralli, and K. Nagayashi
NWO-I/SRON Netherlands Institute for Space Research, Niels Bohrweg 4, 2333 CA Leiden, Netherlands

A. Kozorezov
Department of Physics, Lancaster University, LA1 4YB Lancaster, United Kingdom

(Received 22 December 2020; accepted 12 April 2021; published 26 May 2021)

We present a detailed analysis of the fundamental noise sources in superconducting transition-edge sensors (TESs), ac voltage biased at MHz frequencies and treated as superconducting weak links. We have studied the noise in the resistive transition as a function of bath temperature of several detectors with different normal resistances and geometries. We show that the "excess" noise, typically observed in the TES electrical bandwidth, can be explained by the equilibrium Johnson noise of the quasiparticles generated within the weak link. The fluctuations at the Josephson frequency and higher harmonics contribute significantly to the measured voltage noise at the detector bandwidth through the nonlinear response of the weak link with a sinusoidal current-phase relation.

DOI: 10.1103/PhysRevLett.126.217001

Superconducting transition-edge sensors (TESs) are very sensitive thermometers used as microcalorimeters and bolometers in ground and space-borne low temperature instruments [1,2]. TESs are, typically, low impedance devices made of a thin superconducting bilayer, with a critical temperature T_c. They operate in the voltage bias regime. Either a constant or an alternating bias voltage is used, depending on the multiplexing read-out scheme. In the frequency division multiplexing (FDM) configuration considered here, the TES is ac voltage biased in the superconducting transition, by means of high- Q LC resonators at frequencies from 1 up to 5 MHz. The underlying physics of TESs has been extensively studied in the past years and the TES response under ac and dc bias is fairly well described for TESs behaving as superconducting weak links [3–6], or affected by the generation of phase-slip lines [7].

The basic theory of a TES is extensively reported elsewhere [1,2,4]. The electrical and thermal equations for a TES are solved exactly in the small signal regime with resistance dependency on temperature T and current I linearly expanded to the first order as $R(I,T) = R_0 + \alpha(R_0/T_0)\delta T + \beta(R_0/I_0)\delta I$. Here, $\alpha = (T/R)(\partial R/\partial T)|_{I_0}$, $\beta = (I/R)(\partial R/\partial I)|_{T_0}$, $\delta T = T - T_0$ and $\delta I = I - I_0$. The α and β parameters can be measured experimentally at the operating point and are used to estimate the detector noise and sensitivity. Three fundamental contributions to the TES noise are generally identified. The first one is called *phonon noise* from thermal fluctuations between the TES-absorber body and the heat bath, with power spectral density given by $S_{\mathrm{ph}} = 4k_B T^2 G_{\mathrm{bath}}[(T_{\mathrm{bath}}/T)^{n+2} + 1]/2$, where G_{bath} is the thermal conductance to the bath at a temperature T_{bath} and n is the exponent depending on the nature of thermal processes involved. This noise is dominant at low frequencies in the detector thermal bandwidth typically below ~200 Hz. The second contribution is the Johnson-Nyquist (JN) noise of the TES biased in the resistive transition. It has been modeled so far as a nonequilibrium Johnson noise (NEJN) with voltage spectral density $S_{V,\mathrm{NEJN}} = 4k_B T \mathrm{Re}(Z_{\mathrm{TES}})(1 + 2\beta)$ [8]. It is suppressed at low frequency by the electrothermal feedback [9] and it becomes significant in the detector electrical band at kHz frequencies. The third noise term is the internal thermal fluctuation noise (ITFN), which is generated by thermal fluctuation between distributed heat capacities internal to the TES-absorber system. It has a power spectral density $S_{\mathrm{ITFN}} = 4k_B T^2 G_{\mathrm{TES}}$, where G_{TES} is the intrinsic thermal conductance of the system. The response of the detector to this noise source is identical to the JN noise, which complicates the identification of the TES noise sources in the electrical bandwidth. The ITFN can be derived from a proper characterization of the thermal circuit [10–14]. In Fig. 1, we show the typical current noise spectrum after demodulation of a MHz biased TES operating at $R/R_N = 20\%$, where R_N is the TES normal resistance. More details on how to derive the total current noise measured in a TES from the noise sources described above are given in the Supplemental Material [15]. So far, the total TES noise in the JN bandwidth has not been fully understood. The residual $M^2 = (S_{V,\mathrm{data}} - S_{V,\mathrm{model}})/S_{V,\mathrm{model}}$ is a convenient way to characterize the "excess" noise. The common practice in the TES literature is to define M^2 with respect to the NEJN, i.e., $S_{V,\mathrm{model}} = S_{V,\mathrm{NEJN}}$ [4,11,14,18].

In this Letter, we study the JN noise in many ac biased TESs with different electrothermal properties. We show that the fluctuation-dissipation theorem generalized for a

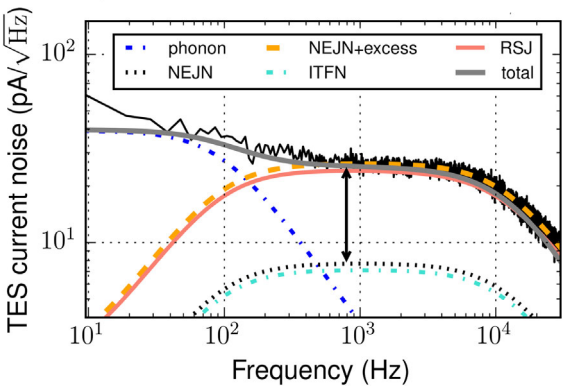

FIG. 1. Current noise spectrum for a TiAu $80 \times 20\ \mu\text{m}^2$ TES biased at 2.6 MHz, $R/R_N = 13\%$ and $T_{\text{bath}} = 55$ mK. The different lines show the noise contributions discussed in the text. The vertical arrow indicates the measured excess noise with respect to the estimated NEJN.

nonlinear system in thermal equilibrium explains well the observed noise and that it is not necessary to introduce the formalism for a nonlinear TES out of equilibrium [8]. The observed spectral density of fluctuations of the TES voltage is in full agreement with the expected equilibrium thermal noise of the quasiparticles. We characterized, at different bias frequencies, many Ti/Au TES microcalorimeters, with critical temperature $T_c \sim 90$ mK, normal sheet resistance $R_\square = 26\ \text{m}\Omega/\square$, and three different geometries (length $\times$ width): 80×40, 80×20, and $120 \times 20\ \mu\text{m}^2$, leading to different values of R_N, α, β, and saturation power. In this way we can probe the noise model in different weak-link regimes [19]. More details on the devices and the read-out system are given in Refs. [15,19]. To study the intrinsic fluctuations inside the TES, we consider the seminal work of Likharev and Semenov [20] and later reviews [21,22]. We consider the resistively shunted junction (RSJ) model previously proposed to explain the excess noise in dc-biased TES [23], extend it to the ac bias case, and provide experimental evidence of its validity. Moreover, as proposed in Refs. [24,25], we compare the RSJ approximation with the generalized kinetic theory for fluctuations in superconductors derived by Kogan and Nagaev (KN) [26] and show that the two models are consistent with each other over a wide range of bias conditions, detector β values, and for different TES geometries. In Ref. [25], only the results for two dc biased TESs are reported and a relatively large discrepancy between the two models is observed. Following the method described in this Letter, the detector noise is accurately estimated since we measure directly the physical quantities required by the RSJ and KN models and no free parameters are left. A fundamental difference between a dc and ac biased TES is given by the evolution of the superconducting phase across the $SS'S$ or S-N-S weak link. Under dc bias, due to the ac Josephson effect, the phase $\varphi(t)$ increases linearly with time at a rate $\omega_J = 2eV_{\text{dc}}/\hbar$ proportional to the bias voltage, where ω_J is the bias dependent Josephson frequency. Under ac bias, on the contrary, $\varphi(t)$ oscillates around an equilibrium value φ_0 at a frequency $\omega_J = \omega_b$, out of phase with respect to the ac bias voltage $V(t) = V_{\text{ac}} \cos(\omega_b t)$, and with a peak amplitude $\varphi_{\text{pk}} = 2eV_{\text{ac}}/\hbar\omega_b$. Despite the difference, when studying the voltage fluctuations within the weak-link context, both the dc and ac biased TES can be seen as a periodical nonstationary system with period $2\pi/\omega_J$. It is then convenient to represent the time dependent system as a combination of Fourier series over frequencies $\omega_m = \omega + m\omega_J$ and solve the problem of the weak-link dynamics as done by Zorin [21,27]. It is shown that the voltage power spectral density of the fluctuation $S_V(\omega)$ is the result of parametric conversion of fluctuations mixed with the Josephson oscillations and its harmonics. The relation with the current power spectrum $S_I(\omega)$ is given by $S_V(\omega) = \sum Z^*_{mm'}(\omega) Z_{mm'}(\omega) S_I(\omega_m)$. Here, $Z_{mm'}(\omega)$ is the impedance matrix of the RSJ, with the indices m and m' standing for the respective harmonics of the Josephson oscillation at ω_J [20,21]. When measuring the noise at $\omega \ll \omega_J$, the contribution from the higher harmonics with $|m| > 1$ was shown to be negligible [28]. The low frequency power spectral density of the voltage fluctuations, averaged over the period of oscillation $2\pi/\omega_J$ for a RSJ can be approximated [15,21,23,29] to

$$S_V(\omega) \simeq R_d^2 \left\{ \frac{3}{2}\frac{R}{R_N}\left[1 - \frac{1}{3}\left(\frac{R}{R_N}\right)^2\right]\right\} S_I(\omega), \qquad (1)$$

where $R_d = \partial V/\partial I = R(1+\beta)$ is the detector dynamic resistance at the bias point. The Equation (1) is valid both for a dc and an ac biased TES [15].

A more general derivation of the spectral density of the voltage fluctuation for a resistively shunted Josephson contact, with arbitrary current-phase relation $I(\varphi)$, has been derived by Nagaev [30]. The calculation is done for a junction biased at a current $I > I_c$ in the region where the quasiparticle distribution function is close to equilibrium and the correlation function of the current is determined by the JN formula. The spectral density $S_V(\omega)$ at frequency $\omega < \omega_J$ is equal to

$$S_V(\omega) = R_d^2 \left[1 - \frac{\hat{V}}{2R_d^2}\frac{\partial R_d}{\partial I}\right] S_I(\omega). \qquad (2)$$

The two terms in the bracket describe the noise of the thermal fluctuations at equilibrium and should be experimentally compared with Eq. (1) derived for a RSJ with sinusoidal current-phase relation. In the derivation of Eqs. (1) and (2), the system is considered to be in thermodynamic equilibrium and the fluctuation-dissipation theorem applies for the thermally excited quasiparticles [31] so that $S_I(\omega) = 4k_B T/\text{Re}(Z_{\text{TES}}(\omega))$, i.e., the TES JN

noise is treated as equilibrium thermal noise with the nonlinearity given by the Josephson impedance Z_{mm}.

The TES electrical noise can be calculated rather precisely from Eqs. (1) and (2) at each bias point after estimating the detector electrothermal parameters. This is done by evaluating the TES complex impedance $Z_{\mathrm{TES}}(\omega, I_0, T_0)$ using the standard technique of measuring the detector current response to a voltage excitation at a given frequency ω. The formalism for a dc and ac biased TES has been described in Refs. [32,33], respectively. The classical expression for $Z_{\mathrm{TES}}(\omega)$ [32] has been modified in Ref. [34] to include the intrinsic reactance predicted by the RSJ model. The details are reviewed in Ref. [15].

The theoretical predictions described above can be verified experimentally. By fitting the complex impedance curves taken along the transition, as described in Ref. [15], we estimate the TES linear parameters α, β, and the detector time constants for many devices and bias frequencies. From β and $R_d = R(1+\beta)$, we calculate for each bias point the total TES voltage spectral density as in Eq. (1).

Evaluating the JN noise from Eq. (2) requires the derivative of the dynamic resistance with respect to the current, which cannot be accurately obtained from the I-V characteristic. Our technique of measuring Z_{TES} provides a straightforward estimation of R_d and $\partial R_d/\partial I$. We use the fact that $\partial R_d/\partial I = -R_d^3 \partial^2 I/\partial V^2$, and that the TES current response to a small and slow modulation $V_m \cos \omega t$ of the voltage bias, with $V_m \ll V_{\mathrm{ac}}$ and $\omega \ll \omega_b$, can be expanded as

$$I(V,t) = I(V) + \frac{\partial I}{\partial V} V_m \cos \omega t + \frac{1}{2}\frac{\partial^2 I}{\partial V^2} V_m^2 \cos^2 \omega t + \cdots \tag{3}$$

The first harmonic is proportional to the inverse of the dynamic resistance $\partial I/\partial V = 1/R_d$, while the second harmonic gives the term $\partial^2 I/\partial V^2$, which is needed to estimate the noise as in Eq. (2). When measuring the intrinsic complex impedance curves, we fit the sinusoidal response up to the third order, to capture the harmonic distortions generated by the Josephson nonlinearity as a function of bias point. An example of the fit of the response to a sinusoidal excitation is shown in Ref. [15]. The coefficient of the first and second order term of the fit is used to accurately estimate the noise from the KN derivation.

We measured the noise for many pixels along the TES resistive transitions. A typical dataset is shown in Fig. 2 for a 80×40 μm TES biased at 2.5 MHz. The voltage noise, measured in the kHz bandwidth, normalized to the thermal noise of resistance $R = \mathrm{Re}(Z_{\mathrm{TES}}(\omega))$, is plotted as a function of R/R_N, along with the different noise contributions. The noise shows the expected oscillating behavior from the Josephson effects being strongly correlated with the TES dynamic resistance. The first main result is that the NEJN dramatically underestimates the noise, in particular at low R/R_N values. The total observed noise is consistent with the prediction from Eq. (1) or Eq. (2), within the 1σ experimental uncertainties indicated by the shaded area around the lines. This result is in agreement with the fluctuation-dissipation theorem generalized for a nonlinear system in thermal equilibrium. The major contribution to the error bars derives from the uncertainties in the estimation of the bias circuit parameters, known within 10%, which propagate in the calculation of V_{TES}, P_{TES}, G_{bath}, α, and β. The second important result is that both the RSJ model and the derivation from KN explain equally well the detector noise. This implies that the sinusoidal current-phase relation assumed in the RSJ model is a good approximation for the detectors and bias conditions discussed here. This is expected when a TES is treated as an S-N-S long diffusive weak link with Thouless energy $E_{\mathrm{TH}} = \hbar D/L^2$, where $D \simeq 0.092$ m^2/s is the diffusion coefficient for Au and $L = 80$–120 μm the TES length, satisfying the condition $E_{\mathrm{TH}} \ll eV \ll k_B T$. The contribution of the ITFN noise for this particular design is typically

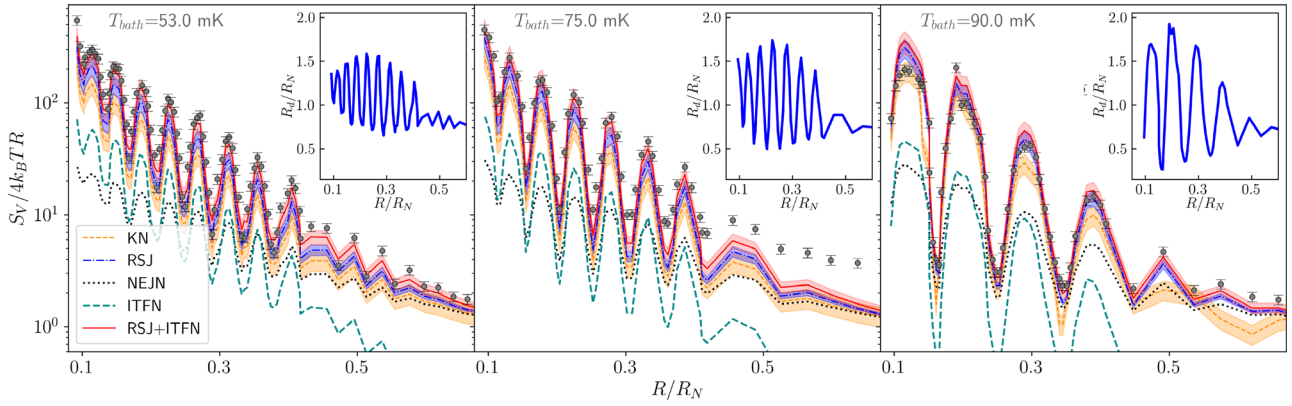

FIG. 2. Measured voltage noise of the 80×40 μm TES as a function of bias point R/R_N. From top to bottom: $T_{\mathrm{bath}} = 53.0$, 75.0, and 90.0 mK. The blue dot-dashed and the orange dashed lines are the prediction from Eqs. (1) and (2), respectively. The green dashed line is the estimated ITFN. The black dotted line is the NEJN. The red line is the sum in quadrature of the RSJ and ITFN noise. Insets: the normalized TES dynamic resistance, $R_d = R(1+\beta)$ as a function of R/R_N.

small, and accounts for about 20% of the total noise. The ITFN is estimated from the Wiedemann-Franz law with $G_{\mathrm{TES}} = L_0 T/R_{\square}$, where L_0 is the Lorenz number [35]. Some excess noise is observed at $R/R_N > 0.4$ for $T_b = 55$ and 75 mK, and it will be discussed later below.

To our knowledge, this is the first time that the general derivation proposed by Nagaev [30] has been experimentally compared against the RSJ prediction. Equation (2) was used before Ref. [24] to explain the shot noise in the coherent regime of long diffusive *S-N-S* junctions at low bias voltage, $eV < E_{\mathrm{TH}}$. In Fig. 3, we summarize the noise measurement done for many other pixels with the three different TES geometries, biased at frequencies from 1.1 to 3.95 MHz. We plot the voltage noise as a function of the factor $1 + 2\beta$ (derived for the NEJN [8]), after subtracting the ITFN contribution. The solid red line is the expected RSJ noise with the shaded area highlighting the 1σ uncertainties. The dashed line is the calculated NEJN. As shown by the small residual M^2 calculated using the RSJ model, the TES JN noise is in very good agreement with the RSJ prediction over a large range of β and for the high and low TES power regime ($T_{\mathrm{bath}} = 53$ and 90 mK, respectively). The measured and expected noise is generally independent of the bias frequency. Excess noise is observed at low value of β ($\lesssim 3$) with some pixels (for example, the 120×20 $\mu\mathrm{m}^2$ biased at 1.1 MHz, and few 80×20 $\mu\mathrm{m}^2$ pixels at a $T_{\mathrm{bath}} = 53$ mK Fig. 3(a)). Figure 4 shows the details of the observed excess noise for two devices as a function of R/R_N and T_{bath}. This noise is reduced when operating the device close to T_c, i.e., at lower TES current [15]. We believe this noise is of a different nature than the noise discussed above, which depends on the TES R, β, and T and not on the current [Eq. (1)]. It is likely due to a nonuniform current and temperature distribution inside the TES caused by the presence of normal metal structures (the stems connecting the absorber [15]) in the current path. The effect is minimized when operating

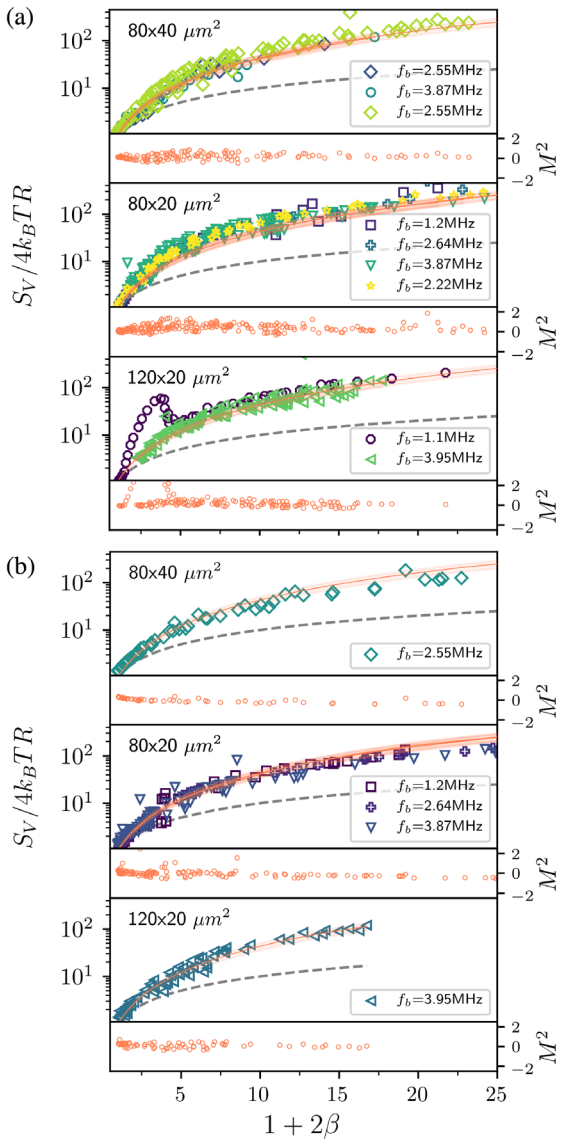

FIG. 3. Voltage noise, after ITFN subtraction, for three different TES design and several bias frequencies, measured at $T_{\mathrm{bath}} = 53$ mK (a) and $T_{\mathrm{bath}} = 90$ mK (b), respectively. The dashed line shows the noise estimation from NEJN. The red solid line is the prediction from the RSJ noise, with the shaded area indicating the 1σ uncertainty on the calculated noise. The red open circle is the residual M^2 calculated with respect to the RSJ model for all the measured pixels.

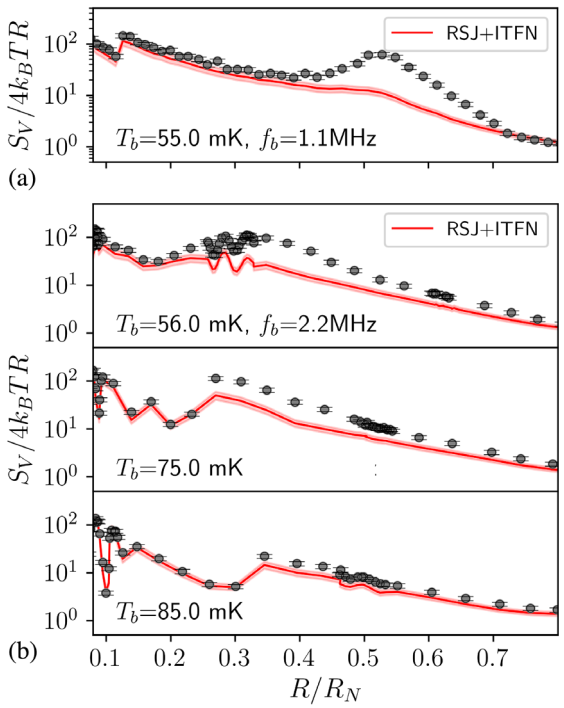

FIG. 4. Measured voltage noise at $T_{\mathrm{bath}} = 55.0$ mK of two 120×20 μm TES as a function of bias point R/R_N biased, respectively, at (a) 1.1 and (b) 2.2 MHz. The latter was measured at (from top to bottom) $T_{\mathrm{bath}} = 56.0$, 75.0 and 85.0 mK. The red curve is the expected RSJ and ITFN noise.

the device close to T_c. From a recent investigation it seems possible to eliminate the excess noise bumps by optimizing the size and the position of the absorber-TES stems. A full study is under way.

In conclusion, we have extensively characterized at MHz bias the voltage fluctuations of TES microcalorimeters with three different geometries and R_N values. When subtracting the expected ITFN noise, the residual noise in the JN bandwidth can be well explained, over a large range of experimental parameters $(R_N, V_{\mathrm{TES}}, f_b, T_{\mathrm{bath}})$, from the theory of noise in Josepshon weak links, following the RSJ model or the more general derivation from KN [26]. The noise is consistent with the equilibrium thermal noise and is enhanced by the nonlinear response of the weak link.

This work is partly funded by European Space Agency (ESA) under ESA CTP Contract No. ITT AO/1-7947/14/NL/BW, by the European Unions Horizon 2020 Program under the AHEAD project (Grant Agreement No. 654215) and is part of the research program Athena (Project No. 184.034.002), which is (partly) financed by the Dutch Research Council (NWO).

*l.gottardi@sron.nl

[1] K. D. Irwin and G. C. Hilton, *Cryogenic Particle Detection* (Springer-Verlag, Berlin, 2005), p. 63149.
[2] J. N. Ullom and D. A. Bennett, Supercond. Sci. Technol. **28**, 084003 (2015).
[3] J. E. Sadleir, S. J. Smith, S. R. Bandler, J. A. Chervenak, and J. R. Clem, Phys. Rev. Lett. **104**, 047003 (2010).
[4] S. J. Smith, J. Adams, C. Bailey, S. R. Bandler, J. A. Chervenak, M. Eckart, F. Finkbeiner, R. Kelley, C. Kilbourne, F. Porter, and J. Sadleir, J. Appl. Phys. **114**, 074513 (2013).
[5] L. Gottardi, S. J. Smith, A. Kozorezov, H. Akamatsu, J. van der Kuur, S. R. Bandler, M. P. Bruijn, J. A. Chervenak *et al.*, J. Low Temp. Phys. **193**, 209 (2018).
[6] L. Gottardi, A. Kozorezov, H. Akamatsu, J. van der Kuur, M. P. Bruijn, R. H. den Hartog, R. Hijmering, P. Khosropanah, C. Lambert, A. J. van der Linden, M. L. Ridder, T. Suzuki, and J. R. Gao, Appl. Phys. Lett. **105**, 162605 (2014).
[7] D. A. Bennett, D. S. Swetz, D. R. Schmidt, and J. N. Ullom, Phys. Rev. B **87**, 020508(R) (2013).
[8] K. Irwin, Nucl. Instrum. Methods Phys. Res., Sect. A **559**, 718 (2006).
[9] K. D. Irwin, Appl. Phys. Lett. **66**, 1998 (1995).
[10] H. F. C. Hoevers, A. C. Bento, M. P. Bruijn, L. Gottardi, M. A. N. Korevaar, W. A. Mels, and P. A. J. de Korte, Appl. Phys. Lett. **77**, 4422 (2000).
[11] Y. Takei, L. Gottardi, H. Hoevers, A. J. de Korte, J. van der Kuur, M. L. Ridder, and M. P. Bruijn, J. Low Temp. Phys. **151**, 161 (2008).
[12] K. M. Kinnunen, M. R. J. Palosaari, and I. J. Maasilta, J. Appl. Phys. **112**, 034515 (2012).
[13] I. J. Maasilta, AIP Adv. **2**, 042110 (2012).
[14] N. A. Wakeham, J. S. Adams, S. R. Bandler, S. Beaumont, J. A. Chervenak, A. M. Datesman, M. E. Eckart, F. M. Finkbeiner, R. Hummatov, R. L. Kelley, C. A. Kilbourne, A. R. Miniussi, F. S. Porter, J. E. Sadleir, K. Sakai, S. J. Smith, and E. J. Wassell, J. Appl. Phys. **125**, 164503 (2019); J. Low Temp. Phys. **200**, 192 (2020).
[15] See Supplemental Material at http://link.aps.org/supplemental/10.1103/PhysRevLett.126.217001 for more details on the electro-thermal circuit and the derivation of the impedance and the noise equations of a TES behaving as a weak link, which includes Refs. [16,17].
[16] C. Kirsch, L. Gottardi, M. Lorenz, T. Dauser, R. den Hartog, B. Jackson, P. Peille, S. Smith, and J. Wilms, J. Low Temp. Phys. **199**, 569 (2020).
[17] W. T. Coffey, J. L. Dejardin, and Y. P. Kalmykov, Phys. Rev. B **62**, 3480 (2000).
[18] J. Ullom, W. Doriese, G. Hilton, J. Beall, S. Deiker, K. Irwin, C. Reintsema, L. Vale, and Y. Xu, Nucl. Instrum. Methods Phys. Res., Sect. A **520**, 333 (2004).
[19] M. de Wit, L. Gottardi, E. Taralli, K. Nagayoshi, M. L. Ridder, H. Akamatsu, M. P. Bruijn, M. DAndrea, J. van der Kuur, K. Ravensberg, D. Vaccaro, S. Visser, J. R. Gao, and J.-W. A. den Herder, J. Appl. Phys. **128**, 224501 (2020).
[20] K. Likharev and V. Semenow, Sov. Phys. JEPT Lett. **15**, 442 (1972).
[21] S. Kogan, *Electronic Noise and Fluctuations in Solids*, 1st ed. (Cambridge University Press, USA, 2008).
[22] A. Vystavkin, V. Gubankov, L. Kuzmin, K. Likharev, V. Migulin, and V. Semenov, Rev. Phys. Appl. **9**, 79 (1974).
[23] A. Kozorezov, A. Golubov, D. Martin, P. de Korte, M. Lindeman, R. Hijmering, J. van der Kuur, H. Hoevers, L. Gottardi, M. Kupriyanov, and J. Wigmore, J. Low Temp. Phys. **167**, 108 (2012).
[24] E. Lhotel, O. Coupiac, F. Lefloch, H. Courtois, and M. Sanquer, Phys. Rev. Lett. **99**, 117002 (2007).
[25] A. Wessels, K. Morgan, D. T. Becker, J. D. Gard, G. C. Hilton, J. A. B. Mates, C. D. Reintsema, D. R. Schmidt, D. S. Swetz, J. N. Ullom, L. R. Vale, and D. A. Bennett, arXiv:1907.11343.
[26] S. M. Kogan and K. Nagaev, Zh. Eksp. Teor. Fiz. **94**, 262 (1988).
[27] A. B. Zorin, Physica (Amsterdam) **108B+C**, 1293 (1981).
[28] R. H. Koch, D. J. Van Harlingen, and J. Clarke, Phys. Rev. B **26**, 74 (1982).
[29] L. G. Aslamazov and A. I. Larkin, Sov. JETP Lett. **9**, 87 (1969), https://ui.adsabs.harvard.edu/abs/1969JETPL...9...87A.
[30] K. E. Nagaev, Sov. Phys. JETP **67**, 579 (1988).
[31] D. Rogovin and D. Scalapino, Ann. Phys. (N.Y.) **86**, 1 (1974).
[32] M. A. Lindeman, S. Bandler, R. P. Brekosky, J. A. Chervenak, E. Figueroa-Feliciano, F. M. Finkbeiner, M. J. Li, and C. A. Kilbourne, Rev. Sci. Instrum. **75**, 1283 (2004).
[33] E. Taralli, P. Khosropanah, L. Gottardi, K. Nagayoshi, M. L. Ridder, M. P. Bruijn, and J. R. Gao, AIP Adv. **9**, 045324 (2019).
[34] A. Kozorezov, A. A. Golubov, D. Martin, P. de Korte, M. Lindeman, R. Hijmering, J. van der Kuur, H. Hoevers, L. Gottardi, M. Kupriyanov, and J. Wigmore, Appl. Phys. Lett. **99**, 063503 (2011).
[35] The internal thermal conductance in a long *S-N-S* junction is not trivial to calculate and it is likely changing along the transition. Assuming that G_{WF} depends on $R_{\square}$ gives typically the best noise estimation over the whole transition in our TESs. The noise, in particular at low TES resistance biasing, turns out to be overestimated when G_{WF} is calculated using R_N as in Ref. [14].